Environmental and Experimental Botany 155 (2018) 165–176

Contents lists available at ScienceDirect

Environmental and Experimental Botany

journal homepage: www.elsevier.com/locate/envexpbot

Early responses to Fe-deficiency distinguish *Sorghum bicolor* genotypes with contrasting alkalinity tolerance

Dario Fernando Luna[a,*], Amalia Beatriz Saavedra Pons[a], Dolores Bustos[a], Edith Taleisnik[a,b]

[a] Instituto de Fisiología y Recursos Genéticos Vegetales - Centro de Investigaciones Agropecuarias (IFRGV-CIAP, formerly IFFIVE) INTA (Instituto Nacional de Tecnología Agropecuaria), Camino a 60 Cuadras, Km 5.5, X5020ICA Córdoba, Argentina
[b] CONICET, Consejo de Investigaciones Científicas y Técnicas de la República Argentina, Argentina

ARTICLE INFO

Keywords:
Sorghum bicolor
Alkalinity tolerance
Fe-deficiency
Chlorophyll fluorescence
OJIP parameters
Phytosiderophores

ABSTRACT

Soil alkalinity is a significant limitation to agricultural productivity and it is associated to several soil features, among them, Fe deficiencies. In this work, we explored the hypothesis that alkalinity tolerance in *Sorghum bicolor* is related to Fe-deficiency tolerance and its underlying mechanisms. An initial screening involving 8 sorghum genotypes identified two with contrasting growth responses to alkalinity (susceptible Minu II and more tolerant Silero INTA Pemán) that were subsequently studied under Fe-deprivation (-Fe) conditions. *Sorghum sudanense* (sudangrass) was included as control tolerant species for Fe deficiency. Growth in hydroponics and in soil indicated that responses to both alkaline and -Fe substrates followed parallel trends in the three genotypes: Minu II was the most sensitive, followed by Silero and sudangrass. Decreases in carbon fixation (*A*) and stomatal conductance were observed earlier in -Fe than in alkalinity, and the intensity in the three genotypes followed the same tendency as growth depressions. Calculations derived from the analysis of *A* as a function of internal CO_2 concentration (A/C_i curves) indicated increased C_i concentration along with a decrease in the efficiency of phosphoenol pyruvate caboxylase activity in Minu II. Fast chlorophyll a fluorescence transients (OJIP-test) revealed decreased PSII connectivity in both Minu II and Silero under -Fe, but Minu II disclosed more damage to the oxygen evolving complex under alkalinity, while sudangrass was largely unresponsive. Expression of the genes for phytosiderophore (Phys) synthesis and transport genes was induced under both alkalinity and -Fe conditions in both *S. bicolor* genotypes, and more strongly in Silero than in Minu II. Lower induction of gene expression in Minu II may be related to its sensitivity to alkalinity conditions associated to reduced Fe availability, leading to alteration in photochemical and biochemical reactions involving Fe. Thus, our results provide support to the concept that susceptibility to Fe-deficiency and alkalinity conditions are associated in *Sorghum bicolor* and highlight some of the physiological traits that underlie this association.

1. Introduction

Recent estimates suggest that, globally, about 412 million ha are affected by salinity and 618 million ha by alkalinity, and both types overlap in some areas (FAO and ITPS, 2015). Soil alkalinity is mainly associated to high HCO_3^- and CO_3^{2-} concentrations (Mengel et al., 1984), a high percentage of exchangeable sodium (ESP > 15%), limited water and air mobility and storage, intensive colloid eluviation and dispersion of organic matter (Rengasamy et al., 2016). Nutrient imbalance, specifically micronutrient deficiencies (Fe and Zn) are also typical features of alkaline soils (Marschner, 1995); and all these features are jointly responsible for the restricted agricultural productivity of alkaline soils. Therefore, it is expected that plants that can efficiently acquire the sparingly soluble Fe in alkaline substrates, that is, Fe-deficiency tolerant plants, will express more alkalinity tolerance (Kawai et al., 1988; Singh et al., 1993; Murata et al., 2015).

Sorghum [*Sorghum bicolor* (L.) Moench] is the fifth most important cereal crop after rice, wheat, maize, and barley (Reddy, 2017). It is a multipurpose crop used for food, feed, fodder and fuel production (Rao et al., 2016); its C4 metabolism supports high temperatures and water limited environments, and it is exceptionally efficient in the use of radiation, water and nitrogen (Rooney, 2014). Notwithstanding the remarkable ability of sorghum to adapt to unfavorable environmental conditions (Zhao et al., 2014), its tolerance to alkaline soils is relatively limited (Römheld and Marschner, 1990) and it is also susceptible to Fe deficiency (Mikami et al., 2011). In this work, we explored the hypothesis that alkalinity tolerance in sorghum is related to Fe-deficiency tolerance and its underlying mechanisms.

* Corresponding author.
E-mail address: luna.fernando@inta.gob.ar (D.F. Luna).

https://doi.org/10.1016/j.envexpbot.2018.06.030
Received 28 March 2018; Received in revised form 22 June 2018; Accepted 24 June 2018
Available online 28 June 2018

Sorghum sudanense, known as Sudan grass or sudangrass, is used for sorghum genetic improvement. *Sorghum*-sudangrass hybrids can tolerate soils with high pH (Clark, 2007). It has been reported that photosynthesis under Fe-limited conditions is less negatively affected in sudangrass than in *S. bicolor* (Clark et al., 1988; Kobayashi and Nishizawa, 2012) and it was used as a Fe-deficiency tolerant control in this work.

Photosynthesis is among the major processes affected by stress conditions that result in reduced growth (Chaves et al., 2009). While much work has focused on salt-stress related photosynthetic responses in plants, relatively little has been contributed to understand the causes for alterations in photosynthesis in plants growing in alkaline soils. The response of photosynthesis (A) to the variation of the internal CO_2 concentration (C_i), A/C_i analysis, has been used to evaluate the contribution of biochemical and stomatal alterations to overall photosynthetic reductions observed under stress (Flexas et al., 2004). Such analysis (Farquhar et al., 1980) has successfully been used in C3 plants to estimate photosynthetic parameters, such as maximum carboxyation rate (V_{cmax},), rate of photosynthetic electron transport (J), triose phosphate use (TPU), etc. However, for C4 plants, due to distinct anatomical and metabolic features, the original Farquhar model was found to be inadequate for the estimation of some of these parameters (Collatz et al., 1992) and several corrections have been proposed to adapt this analysis to C4 plants (Bellasio et al., 2016; Ubierna et al., 2013; Yin et al., 2011). To understand the physiological basis for alkalinity limitations to photosynthetic activity in sorghum, in the current work, a detailed analysis of the A/C_i response curves was performed as suggested by Zhou et al., (2017) and C4 photosynthetic parameters such as CO_2-saturated photosynthetic rate (V_{pr}), efficiency of PEPc (CE), the ratio C_i/C_a, were estimated following Naidu and Long (2004).

Chlorophyll a fluorescence (ChlF) transient is very rich in information regarding the physiological state of the electron transport components of PSII and PSI (Bussotti, 2010; Mamedov et al., 2015). If plotted on a logarithmic time scale, ChlF transient shows a polyphasic shape (Kautsky effect). Phases are termed O-J-I-P; where O is the minimal fluorescence (Fo), P is the maximum fluorescence at about 300 ms (Fp), and J and I are intermediates inflection points (Strasser and Srivastava, 1995). The analysis of OJIP curves has provided valuable information for understanding the effects of a wide range of environmental stresses on the photosynthetic electron transport chain (Kalaji et al., 2014; Kaňa and Govindjee, 2016; Roháček et al., 2008) Recent studies have demonstrated that under some stress conditions, such as drought and heat, other steps can appear in fluorescence transients, known as K and L-bands (Oukarroum et al., 2007; Strasser et al., 2004), providing information on the electron flow from the oxygen evolving complex (OEC) to the PSII reaction centers (RC) (Strasser et al., 2004) and the energetic connectivity between PSII units. An OJIP analysis was performed in this work to elucidate the effects of alkalinity and Fe deficit on photosynthetic electron transport.

As indicated earlier, Fe deficiencies are typical features of alkaline soils (Marschner, 1995). When Fe is limited in the substrate, and depending on the kind of plant, roots rely on two main strategies/processes to capture it (Kobayashi et al., 2014). Strategy I is present in most non-graminaceous species. This mechanism includes the activation of three reactions: (i) proton excretion (via P-type ATPase) (ii) reduction of Fe^{3+} by a Fe^{3+}-chelate reductase (iii) plasmalemma transport of Fe^{2+} by iron transporters (Hell and Stephan, 2003). Grasses, on the other hand, use Strategy II to efficiently acquire the sparingly soluble Fe^{3+}, this strategy has been shown to be more efficient than Strategy I in calcareous soils (Römheld, 1987). Strategy II comprises the synthesis and secretion of mugineic acids (MAs) (Kawai et al., 1988; Marschner et al., 1986), which are non-proteinogenic amino acids of low molecular weight with six functional groups for Fe chelation, collectively known as phytosiderophores (Phys). All the MAs described so far derive from the same precursor: methionine (Curie et al., 2009) which is adenosylated by S-adenosylmethionine synthase (SAM). Then, nicotianamine synthase (NAS) catalyzes the trimerization of SAM to nicotianamine (NA; Higuchi et al., 1994). Next, NA aminotransferase (NAAT) catalyzes the transamination of NA to produce the 3''-oxo intermediate (Kanazawa et al., 1995). Finally, DMA synthase (DMAS) reduces the 3''-oxo form to DMA (2′-deoxymugineic acid) (Inoue et al., 2008). In rice, barley and maize, the release of Phys is carried out by the TOM transporter (Nozoye et al., 2011) and, subsequently, Fe-Phys complexes are taken up by the root through a proton-coupled symporter called Yellow Stripe Like (YSL) (Curie et al., 2001). The genes encoding Phys biosynthetic enzymes as well as those for Fe-Phys release and uptake transporters, have been isolated from barley, maize, and rice (Inoue et al., 2008; Kobayashi et al., 2008; Mori, 1999), however, in sorghum and sudangrass, the expression of such genes under alkaline and/or Fe deprivation conditions had not been previously assessed.

These two aspects, the analysis of photosynthetic alterations induced by alkaline and -Fe stress and the expression of genes that encode for proteins that participate in the synthesis, release and uptake of Phys, were included in this work. They were compared in *S. bicolor* genotypes with contrasting alkalinity tolerance and sudangrass.

2. Materials and methods

2.1. Trials and setup

2.1.1. Identifying sorghum genotypes with contrasting alkalinity tolerance

The purpose of the trials described in this section was to identify genotypes with contrasting growth responses to alkalinity that were subsequently studied under Fe-deficiency conditions. The initial screening for alkalinity tolerance was carried out in hydroponics (Experiment 1), and the relative performance of contrasting genotypes was validated in soil (Experiment 2). All trials were carried out in a naturally illuminated greenhouse, supplemented with Powerstar HQI-T 400 W/D (OSRAM) lamps set to a 16 h photoperiod. Seeds were provided by Dr. Laura M. Giorda, Estación Experimental Manfredi – INTA, Córdoba, Argentina and by Oscar Pemán SA,

Experiment 1. Alkalinity tolerance screening in hydroponics. Eight *S. bicolor* genotypes (MINU II, A103385, RMF32, BMF80, Antel, AMF587, Escobero Petaco and Silero INTA Pemán), were tested. Four seeds were sown in 2 L perforated plastic pots, filled with a 2:1 mix of sand and perlite and two seedlings per pot remained after thinning for homogeneity when plants had 1–2 leaves. The pots were sub irrigated with half-strength nutrient solution (Hoagland and Arnon, 1950), pH 6.50 or 8.75, every four hours, by means of an automatic irrigation system. The alkaline treatment was prepared by adding 10 mM $NaHCO_3$ and 2 mM Na_2CO_3 to the nutrient solution. The trial was laid out in a randomized complete block design with six blocks per treatment. It was repeated two times, with similar results; those from the first trial are shown.

Plants were harvested when controls had four completely developed leaves, dried at 75 °C for two days and subsequently weighed. Alkalinity tolerance was assessed from the ratio of plant weight in alkaline to neutral substrate.

Experiment 2. Performance of two contrasting *S. bicolor* genotypes and sudangrass in alkaline and neutral soil, both silt-loamy soils. Two *S. bicolor* genotypes (Silero INTA-Pemán and MINU II), which had shown contrasting responses to alkalinity stress in the previous trials and *S. sudanense* variety MF Sudan 7 INTA, were tested in soil to verify whether the differences in alkalinity tolerance observed in hydroponics, matched the tolerance to alkaline soil and if sudangrass expressed the expected higher alkalinity tolerance. Soil analyses are given in Supplementary Table 1. According to the EC of the alkaline soil (< 4) and the exchangeable Na percentage (ESP > 15), this soil is classified as sodic. Plants were grown in the same greenhouse mentioned above.

Fifteen seeds per genotype were sown in 3 L pots containing neutral or alkaline (sodic) soil. Emergence percentage was calculated ten days after sowing. After emergence assessment, plants were thinned to one per pot to evaluate growth, ion concentration and carbon fixation (A/C_i

curves, see details further down). Plants were harvested 45 days after sowing, dried at 75 °C for 48 h and subsequently weighed.

2.1.2. Alkalinity and Fe-deficiency tolerance in two contrasting S. bicolor genotypes and sudangrass (Experiment 3, hydroponics)

The next step was to test the hypothesis that alkalinity tolerance is related to Fe-deficiency tolerance. For this purpose, plants were grown on neutral, alkaline and neutral solutions lacking Fe.

Seeds were disinfected in sodium hypochlorite (3%, v/v) during 20 min, rinsed and laid on humid filter paper at 27 °C, in a growth chamber. Germinated seeds were placed in nets covered with vermiculite, over 3.8 L containers with aerated distilled water. Upon emergence (approximately 5 days later), the distilled water was replaced by half-strength Hoagland solution pH 6.5. After five more days, plants were divided into three groups: complete half-strength Hoagland solutions (pH 6.5 and 8.75) and pH 6.5 solution lacking Fe (without 100 µm M $C_{10}H_{12}N_2NaFeO_8$).

The solutions were renewed every five days and the pH was monitored periodically.

Plant shoots were harvested after 15 days of treatment, oven-dried at 75 °C for two days until constant weight and weighed. Photosynthesis, chlorophyll fluorescence rise kinetics and gene expression related to Phys production, release and uptake were measured, as detailed further down. The experiment was repeated twice.

2.2. Plant analyses

2.2.1. Ion concentration

Concentration of several cations (Na^+, K^+, NH_4^+) and anions (NO_3^-, PO_4^{3-}, SO_4^{2-}) were assessed in mature leaf blades from Experiment 2, at harvest. Approximately 50 mg of leaf tissue per sample were ground in liquid nitrogen and subsequently suspended in 0.1 N HNO_3. Ions were determined by HPLC (Shimadzu Prominence Modular HPLC, Kyoto, Japan) and concentrations were calculated on a dry weight (DW) basis. Cations were determined using a Shim-pack IC-C3 (Shimadzu Co.) column with IC-C3G guard column. A filtered and degassed 3 mM oxalic acid solution was used as eluent. Each run was performed at 40 °C. flow rate was 1.2 ml/min, during 18 min, without suppression. Anions were determined with a Shim-pack IC-SA3 column along its correspondent precolumn. As eluent, a filtered and degassed 3.6 mM Na_2CO_3 solution was used. Runs were performed at 45 °C, 0.8 ml/min flow rate, during 22 min, using cationic suppression. The detection was performed by conductimetry. Chromatographs were registered and analyzed using LabSolutions (ver.5.6) software. The content of Fe^{2+} in leaves was assessed in plants from Experiment 3, following Campestre et al., (2016). The youngest emerged leaves were harvested on day 6 of treatment, washed with deionized water, frozen in liquid N_2, and stored at −80 °C until analysis. Approximately 100 mg per sample were suspended in 1.2 mL of 80 mM 2.2-dipyridyl-HCl (pH 3.0) in 10% methanol and mixed for 24 h in the dark. Extracts were passed through a 0.45 µm syringe filter, and absorbance at 522 nm was determined with a Beckman DU-640 spectrophotometer (Beckman Instruments Inc., Fullerton, CA, USA).

2.2.2. Carbon fixation and chlorophyll fluorescence

2.2.2.1. Net photosynthesis rates. Net CO_2 assimilation rates were measured in the youngest fully expanded leaves of plants from all experiments with a portable photosynthesis system LI-6400 XT equipped with a LED leaf cuvette (Li-Cor, Lincoln, NE, USA). Results from Experiments 2 and 3 are presented. Environmental conditions inside the cuvette were set as follows: ambient CO_2 concentration was kept at 400 µmol CO_2 mol^{-1}; internal LED light source was set at saturating incident photosynthetic photon flux density (PPFD) of 1500 µmol m^{-2} s^{-1} and the temperature at 25 °C.

2.2.2.2. Carbon fixation as a function of the internal CO_2 concentration (A/C_i response curves). These responses were measured in the youngest fully expanded leaf of plants from Experiment 2, using the equipment and settings mentioned above. The measurements were taken at the end of trial in soil (45 days after the sowing). We performed intensive A/C_i curves as recommended by (Zhou et al., 2017) for C4 species. The reference CO_2 concentrations were set as follows: 400, 200, 50, 125, 150, 175, 200, 225, 250, 275, 300, 325, 350, 400, 500, 600, 700, 800, 1000, 1200, 1400 ppm. The carboxylation efficiency (CE) of phosphoenol pyruvate carboxylase (PEPc) was calculated as the initial slope of A/C_i curves ($C_i < 100$ ppm). The CO_2-saturated photosynthetic rate (V_{pr}) was estimated from the horizontal asymptote of A/C_i curves (Naidu and Long, 2004). The ratio between the ambient CO_2 (C_a), when $CO_2 = 400$ ppm, and the internal CO_2 (C_i) was also calculated (Tan et al., 2017).

2.2.2.3. Chlorophyll a Fluorescence rise kinetics (OJIP-Test). Chlorophyll fluorescence emission was measured with a Pocket-PEA fluorometer (Plant Efficiency Analyzer, Hansatech Instruments Ltd., King's Lynn, Norfolk, UK) as described by Strasser et al., (2004), in plants from Experiment 3. Before measurements were taken, the youngest fully developed leaves were dark-adapted by shuttered leaf clips for at least 30 min in order to allow for full oxidation of the reaction centers (RC). The fluorescence curves (OJIP) were induced by the application of a 1-second light pulse of 3500 µmol m^{-2} s^{-1} in the 650 nm spectrum band. For nomenclature please refer to Supplementary Table 2. For calculation of the OJIP parameters (Supplementary Table 2), the extremes and intermediate fluorescence levels of the original data were used. From these fluorescence values, a set of parameters were calculated to identify the damage site on the electron acceptor site of PSII according to the OJIP-test equations (Strasser et al., 2004). Changes in the oxygen evolving complex activity (OEC) and in the connectivity at PSII were calculated according to Oukarroum et al. (2007) and Gururani et al. (2015). To reveal changes in OEC (K-band), fluorescence curves were normalized at both the O and P steps rendering W_{OP} curves. Next, W_{OP} curves from control plants were subtracted from treated ones ($W_{OP(Treated)}$ - $W_{OP(Control)}$) to disclose bands. Positive values in these bands denote damage to the OEC. To detect L bands, curves were normalized between 0 and 300 µs, and plotted as W_{OK} curves. Plotting the subtraction between $W_{OK(Treated)}$ - $W_{OK(Control)}$ values allowed the visualization of L bands, where positive values are proportional to the loss of connectivity at PSII.

2.2.3. Expression of Phys-related genes

These assays were performed in plants from Experiment 3.

2.2.3.1. Identification of NAS2, NAAT1, DMAS1, TOM1 and YSL1 homologous genes in sorghum. Similarity searches were carried out using genomic sequences of maize: ZmNAS2; (GRMZM2G124785), ZmNAAT1 (GRMZM2G096958), ZmDMAS1 (GRMZM2G060952), ZmTOM1 (GRMZM2G063306), and ZmYS1 (GRMZM2G156599) as queries against Phytozome v12.1 (https://phytozome.jgi.doe.gov/pz/portal.html) and Gramene (http://ensembl.gramene.org/genome_browser/index.html) databases for sorghum potential homologous genes. Reciprocal BLAST (Basic Local Alignment Search Tool) search engine (https://blast.ncbi.nlm.nih.gov/Blast.cgi) has also been performed to ensure the unique relationship between the orthologous genes. The matching sorghum mRNAs having good coverage, identity > 85% and E-value = 0.0 were considered significant. *Sorghum* homologous sequences were acquired and then used to conduct BLASTP in *Zea mays* database. Specific primers were designed from each target sequence using Primer-BLAST. (https://www.ncbi.nlm.nih.gov/tools/primer-blast/) and AmplifiX v.1.7.0 (http://crn2m.univ-mrs.fr/pub/amplifix) and used to conduct

Table 1
Real time RT-PCR results of the expression of the Phys-related genes on day six of treatment.

Gene name	Primer sequence (5'-3')	Product size (bp)	qPCR efficiency (%)	*Genotypes*	*Log2 (Ratio) Stress/control*		R^2	*p-value*	
					Alk	*-Fe*		*Alc*	*-Fe*
SbNAS2	Forward TTGATCCCGAGGACATCCGT	125	91.4	Minu II	1.91	3.8	0.996	0.0585	0.0042
	Reverse AGAAACCTCCGTCTTTGCGT			Silero	3.44	3.46		0.003	0.0014
				sudangrass	0.3	0.82		0.254	0.0734
SbNAAT1	Forward GCACACTTGGACCACACCAAAC	135	101.2	Minu II	1.14	3.28	0.991	0.756	0.0083
	Reverse ATGGGATGGGCAAACGCAAAC			Silero	3.22	3.5		0.0014	0.0022
				sudangrass	1.18	1.95		0.1176	0.0288
SbDMAS1	Forward AGATCAACCCAGTGTGGCAG	131	89.5	Minu II	0.98	2.09	0.998	0.0388	0.001
	Reverse ACCAGAGTCCATCACCGAGT			Silero	2.17	1.91		0.0005	0.0005
				sudangrass	0.38	0.47		0.05	0.0409
SbTOM1	Forward TGCAGGTGCTGGACTTATTGT	117	108.8	Minu II	2.35	5.11	1.00	0.1164	0.0081
	Reverse GCAGCGATAAGTGGTACGGA			Silero	3.72	4.69		0.0138	0.0081
				sudangrass	0.44	1.99		0.3081	0.0246
SbYSL1	Forward CATGAAGTTCACGCCTGGAAG	174	96.9	Minu II	1.61	2.99	0.989	0.1649	0.0304
	Reverse TCTCGGAGAAGGAGAACCCA			Silero	0.65	0.69		0.316	0.2267
				sudangrass	0.13	0.3		0.4469	0.3765

semiquantitative RT-PCR or quantitative real-time PCR. All primers used are listed in Table 1 and were ordered from Ruralex (Buenos Aires, Argentina). The amplified products sizes were confirmed by agarose gel electrophoresis and after its purification were sequenced for real sequences.

2.2.3.2. RNA isolation, semiquantitative RT-PCR and real-time RT-PCR. Root tissues of seedlings from Experiment 3 were used for RNA isolation. Sampling time for gene expression was determined in a preliminary experiment using semiquantitative RT-PCR analysis. After the onset of Fe deficiency plants were sampled 2, 4, 6, 10 and 14 d after the initiation of the -Fe treatment. Results indicated that maximum expression for the studied genes was observed on day 6. Root tips (30–40 per sample) were harvested when plants were in the sixth day of the Fe-deficiency treatment, and immediately frozen in liquid nitrogen and stored at −80 °C for further use. First-strand cDNA was synthesized using M-MLV (Promega) according to the manufacturer instructions. In a total reaction volume of 25 µL, 2 µg of total DNase-free RNA was primed with 1 µg d(T)20 (Ruralex). For qPCR, reactions were carried out in a 15-µL reaction mix containing 250 nM of each primer, 1 µL of cDNA sample and iQ SYBR Green Supermix (Bio Rad). Non-template controls were incorporated in each analysis. qPCR reactions were performed using a iQ5 (Bio Rad) thermocycler. The thermal profile was set to 95 °C for 3 min, followed by 40 cycles of 95 °C for 30 s, 61 °C for 30 s, and 72 °C for 30 s. Amplicon specificity was verified by melting curve analysis (55 to 95 °C) after 40 PCR cycles. The qPCR assay was carried out using three biological replicates for each treatment and two technical replicates for each biological replicate.

Serine/threonine-Protein (PP2A) and Eukaryotic Initiation Factor 4 A (ElF4α) genes previously characterized in sorghum (Reddy et al., 2016) were selected as reference genes. Amplification efficiencies were determined for each gene following the recommendations of Svec et al., (2015). The expression profiles of these genes were estimated in relation to reference genes using fg Statistic software following Pfaffl et al., (2002). The data show the relative increase or decrease of the gene expression level in each sample compared to the gene expression levels in control sample in two experimental replicates and three biological replicates. For semiquantitative RT-PCR, 2 µL of 1:20 diluted cDNA was used for each reaction carried out in a volume of 20 µL made using 150 nM of each PCR primer, 100 µM dNTPs, 1X GoTaq reaction buffer and 0.5U GoTaq DNA polymerase (Promega). All PCR products were measured at 28 cycles determined to be non-saturating. PCR was performed using an Eppendorf Mastercycler Gradient thermal cycler (Eppendorf).

2.3. Statistics

Statistical analyses were conducted using InfoStat software, version 2008 (Di Rienzo et al., 2011). Prior to the analysis, the assumption of normality of the variables was checked using the Shapiro-Wilks modified by Rahman and Govindarajulu, (1997). Data were subject to two-ways analysis of variance. Means comparison were performed using *post-hoc* Fisher's LSD (least significant difference) test. Values were considered significant when $p < 0.05$. Principal components analyses (PCA) were performed with results from Experiments 2 and 3.

3. Results

3.1. Identifying sorghum genotypes with contrasting alkalinity tolerance: growth and carbon fixation

After 5 weeks of growth in alkaline medium (pH 8.75), shoot biomass significantly decreased in all the tested sorghum genotypes (Fig. 1). Variability among the genotypes in alkalinity tolerance was observed: Silero INTA-Pemán (termed Silero from here on) was the most tolerant in the group (Fig. 1A). This hybrid also kept higher rates of photosynthesis under alkaline conditions (35% lower than in the control plants, Fig. 1B). In contrast, Minu II had the poorest performance in alkaline solution, both in terms of growth and net CO_2 fixation (Fig. 1A and B).

To verify whether growth and carbon fixation in alkaline nutritive solution positively correlated with those in alkaline (sodic) soil, the contrasting genotypes, along with the sudangrass, were sown in pots containing either neutral or alkaline (sodic) soil. Emergence decreased in alkaline (sodic) soil (Supplementary Fig. 1), the reduction was most severe in Minu II (> 80%), followed by Silero (~40%) while sudangrass was the least affected (~20%).

The growth of Silero and sudangrass was reduced to a similar extent in alkaline (sodic) soil (about 40%) while Minu II was affected by nearly 50% (results not shown). Net carbon fixation in alkaline (sodic) soil reached about 60% of control values in Silero and sudangrass, and only 25% in Minu II (Fig. 2). Stomatal conductance values in alkaline (sodic) soil were higher than 80% of values in neutral soil in Silero and sudangrass and only 47% in Minu II. A/C_i response curves (Fig. 2A, B, C) indicated the CO_2-saturated photosynthetic rate (V_{pr}, calculated as the horizontal asymptote of each A/C_i curve, Fig. 2D) and the carboxylation efficiency of PEPc (CE; Fig. 2E) were reduced in alkaline (sodic) soil in all three genotypes, but more intensively in Minu II, where the C_i/C_a relation was also modified (increased), suggesting mesophyll restrictions to carbon fixation (Fig. 2F).

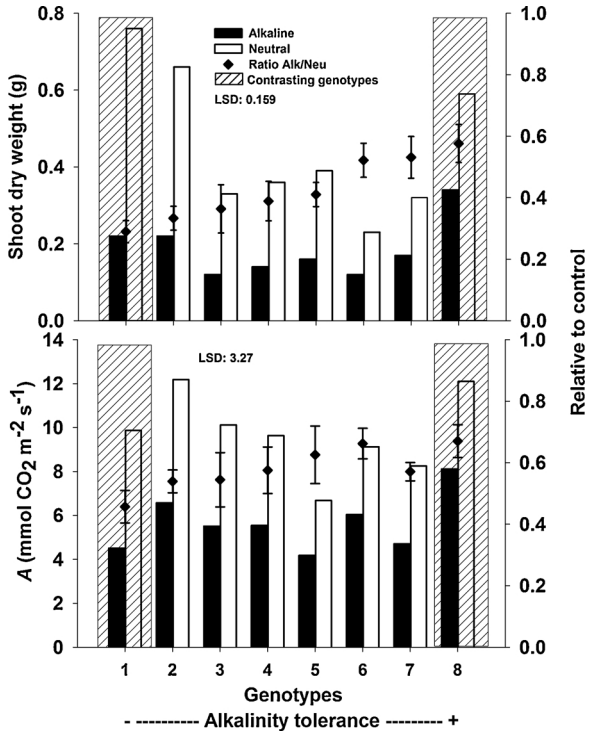

Fig. 1. Effect of alkalinity on growth and carbon fixation in *S. bicolor* genotypes. Upper panel: Shoot dry weight. Lower panel: Net photosynthesis (*A*).
Data were obtained after 45 days of treatment in nutrient solutions pH 6.50 (white bars) or 8.75 (dark bars). LSD for absolute values (left axis) are shown in each panel. The points show average ratios ± SE of alkaline to neutral results (scale on the left axis). Genotypes are 1, Minu II; 2, A103385; 3, RMF32; 4, Antel; 5, AMF587; 6, Escobero Petaco; 7, BMF80 and 8, Silero INTA Pemán. Stripped bars indicate the contrasting genotypes used in subsequent experiments. n = 12.

Ion accumulation analyses (Supplementary Fig. 2) revealed that shoots of *S. bicolor* plants grown in alkaline (sodic) soil accumulated more Na^+ than sudangrass, while K^+ concentrations were not affected by alkalinity. NH_4^+ concentrations decreased in alkaline conditions whereas NO_3^- and SO_4^{-2} increased in all genotypes.

All the above variables were included in a Principal Component Analysis (PCA), and the resulting biplot is shown in Fig. 3. The first Principal Component (PC) separated plants grown in neutral (left side, negative values on the x axis) and alkaline (sodic) soil (on the right), where Minu II appears furthest to the right. Plants in alkaline (sodic) soil negatively correlated to all photosynthetic variables, (which were negatively affected in this condition), except C_i/C_a, which increased, as mentioned earlier. Lower growth in alkaline (sodic) soil was associated to increases in NO_3^-, SO_4^{-2} and Na^+ concentrations.

Together, these results confirmed, in soil, the relative alkalinity tolerance of the *S. bicolor* genotypes observed in nutrient solution, indicating, in addition, that sudangrass, along with Silero, were more tolerant than Minu II.

3.2. Comparison of responses to alkalinity and Fe deprivation

3.2.1. Growth and carbon fixation

It was then enquired whether alkalinity tolerance would match Fe deprivation tolerance. To force differences, Fe was completely omitted from the growth medium after 5 d in full nutrient solutions to sustain initial plant growth.

Cultivation of sorghum and sudangrass seedling in alkaline and Fe-free medium (-Fe) led to a significant reduction in growth (not shown). Fe^{2+} concentration in young leaves had already significantly decreased 5 d after plants were transferred to either alkaline or -Fe medium (Supplementary Table 3). By day 10, Fe deficiency symptoms (chlorosis in the youngest fully expanded leaves, Fig. 4) were evident in -Fe and incipient in the alkaline treatment and were clearly more marked in Minu II than in the other genotypes. Under both alkalinity and -Fe, carbon fixation (*A*) and stomatal conductance (g_s) were negatively affected earlier, and more intensively in Minu II than in the other genotypes (Fig. 5). Thus, tolerance to Fe deprivation in these genotypes followed the same trend as alkalinity tolerance.

3.2.2. PSII electron transport chain

Fast ChlF kinetics analysis, namely an OJIP analysis, reveals alterations in events that concern the electron transport chain at PSII. To provide an overall picture, the original OJIP curves were normalized to their respective controls and plotted as radar graphs (Fig. 6). After 5 days of growth under -Fe conditions most ChlF parameters were altered in Minu II, but the effects of the alkaline medium were less conspicuous. In the -Fe treatment, a significant increase of light energy dissipation as latent heat, (represented by DIo/RC), was observed, while the absolute performance index (PI_{abs}) dropped 72% percent. The F_v/F_m parameter decreased, due to the elevation in the minimum ChlF emission (F_0), rather than the reduction of maximum fluorescence (F_m). The absorption and trapping of energy by reaction centers (ABSo/RC and TRo/RC, respectively) also increased under –Fe condition, while the area (Area) of the OJIP curve was noticeable reduced. In sudangrass almost all the parameters remained unaltered in response to alkaline and –Fe treatments (Fig. 6C), Silero showed intermediate sensitivity both to the alkaline and –Fe media.

Alkalinity stress scarcely affected the oxygen evolving complex (OEC) activity in all genotypes, as reflected in the lack of change in the K bands (Fig. 7, left panels). Minu II exhibited a more pronounced K-band under –Fe conditions than Silero subjected to the same treatment, indicating a higher loss of OEC activity. The energetic connectivity of PSII units, expressed as the W_{OK} and ΔW_{OK} amplitude (L band, Fig. 7, right panels), increased under –Fe and alkaline conditions in both, Minu II and Silero while it remained unaltered in sudangrass.

Taken together, the above results confirmed that Minu II was both more sensitive to alkalinity and Fe-deficiency than the other two genotypes, and indicated that carbon fixation and chlorophyll fluorescence alterations were associated to this sensitivity. Specifically, a significant increase in light energy dissipation (DIo/RC) along with a drop in the performance index (PI) and altered electron transport at PSII resulting from the detected alteration in connectivity at PSII, were observed. Most of these changes were conspicuous at the –Fe treatment and incipient under alkaline conditions.

3.2.3. Alteration in the expression pattern of genes related to Phys production, release and uptake

Next, we explored whether sensitivity to alkaline and Fe-deprived substrates was associated to the expression of genes related to Strategy II Fe uptake mechanisms, namely those involved in Phys production, release and uptake.

Expression of most Phys-related genes increased significantly in comparison to control plants after 6 days of treatment in the two *S. bicolor* genotypes, but there were fewer significant changes in sudangrass and always of less magnitude (Table 1). Comparing Minu II and Silero, expression increases were higher under Fe deprivation than under alkaline conditions, which is to be expected as alkalinity-associated Fe deficiencies would take longer to express than responses to a Fe-free medium. The expression of NAS2, which catalyzes the first step

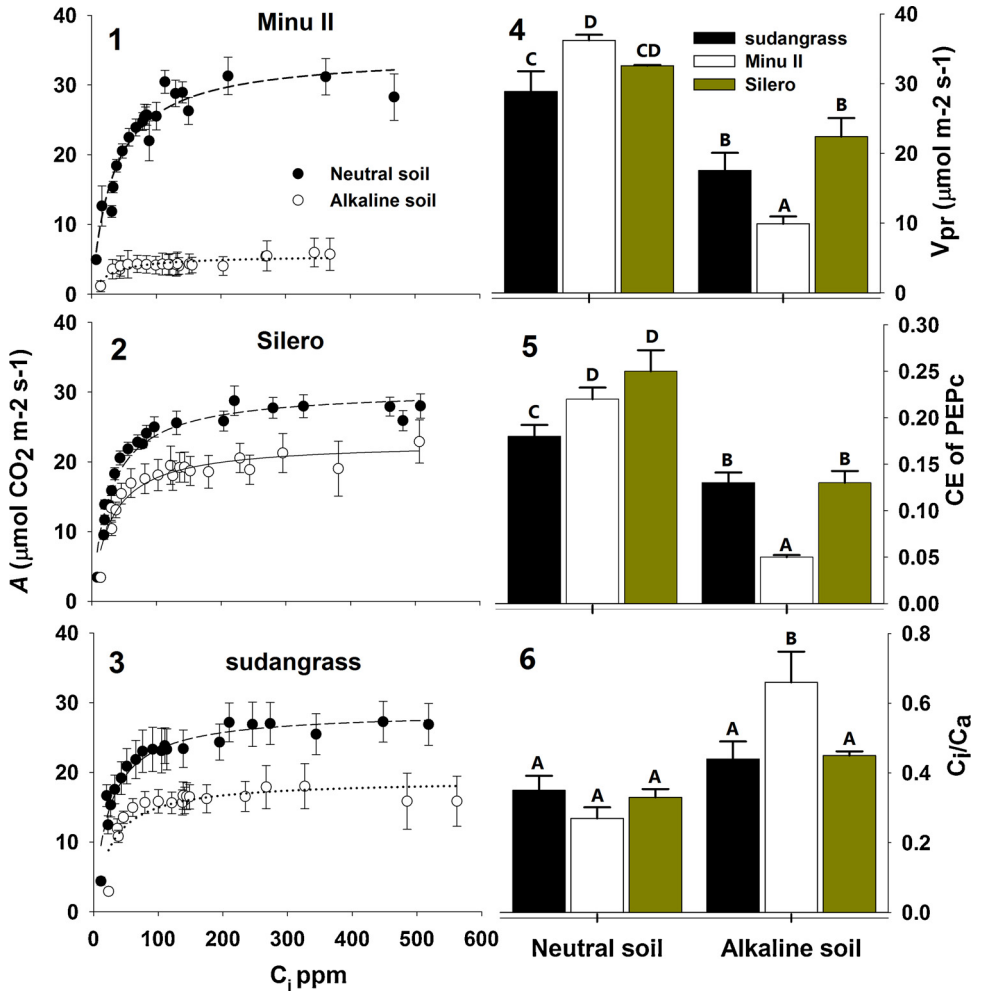

Fig. 2. Alkalinity effects on photosynthetic parameters in sudangrass and two *S. bicolor* genotypes (Minu II and Silero). A to C, Carbon fixation (*A*) in response to a range of internal CO_2 concentrations (C_i) measured on day 45 of growth in neutral (•) or alkaline soil (○). Dots show average ± SE of 4 samples. Parameters in panels D to F were derived from the A/C_i curves. D, CO_2-saturated photosynthetic rate (V_{pr}); E, carboxylation efficiency (CE) of phosphoenol pyruvate carboxylase (PEPc) and F, ratio between internal (C_i) and ambient (C_a, set at 400 ppm) CO_2 concentrations. Different letters indicate significant differences at $p < 0.05$.

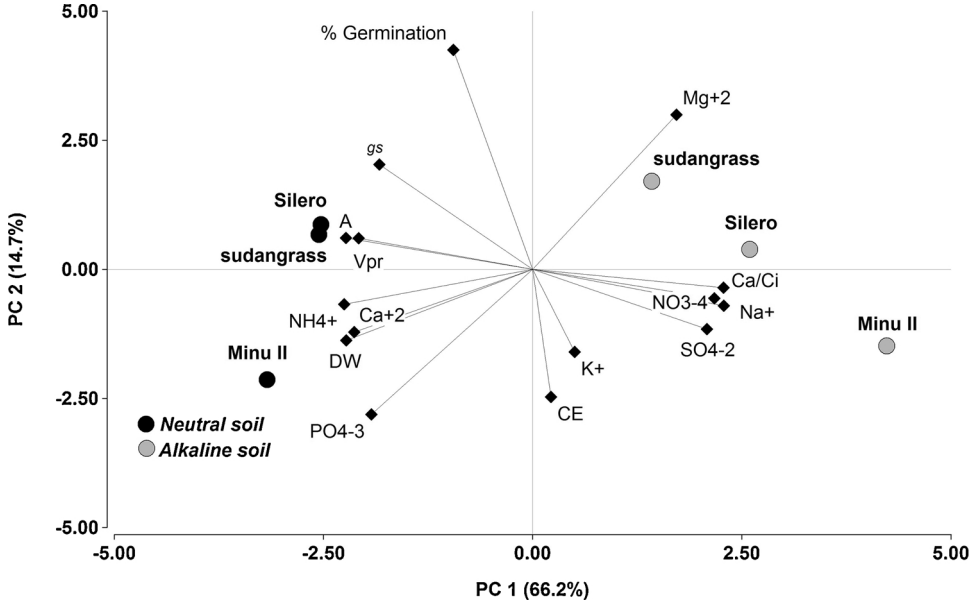

Fig. 3. Biplot of a Principal Component Analysis including germination, growth, ion accumulation and photosynthesis data obtained in alkaline soil. Except for germination the rest of the variables were measured 45 d after sowing in pots containing neutral or alkaline soil. Gray circles: *Sorghum* genotypes in neutral soil, black circles: genotypes in alkaline soils. Vectors represent variables (*A*: Photosynthesis, *gs*: stomatal conductance, V_{pr}: CO_2-saturated photosynthetic rate, DW: dry weight, C_a/C_i: ratio between ambient to internal CO_2 concentration, CE: carboxylation efficiency of phosphoenol pyruvate carboxylase (PEPc), and the rest are ions (PO_4^{-2}, Ca^{+2}, NH_4^{+}, SO_4^{-2}, Mg^{+2}, NO_3-, Na^{+}). Coffenetic correlation coefficient 0.95.

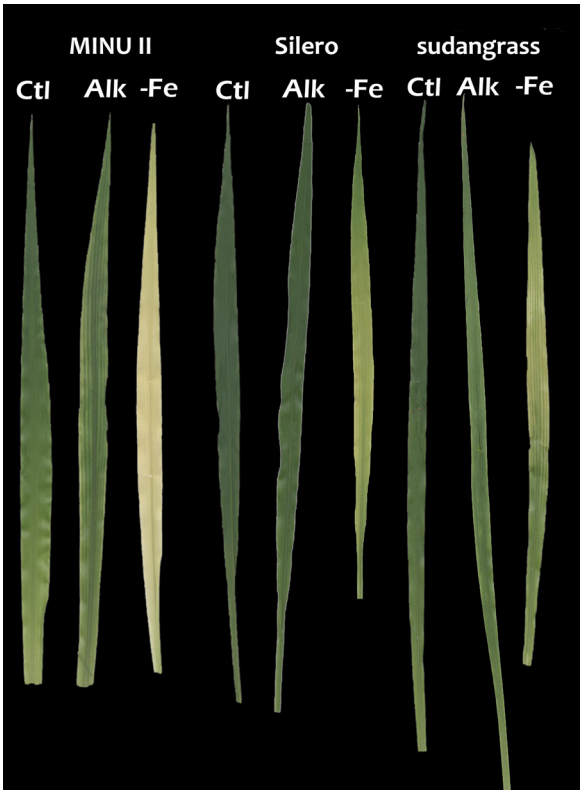

Fig. 4. Chlorosis symptoms in the youngest fully expanded leaves of *S. bicolor* (Minu II and Silero) and sudangrass plants after 10 d of growth in neutral (Ctl), alkaline (Alk) or neutral Fe-deprived (-Fe) nutrient solutions.

in Phys biosynthesis, increased in both Minu II and Silero. The genes encoding for nicotianamine amino transferase (NAAT1) and 2´-deoxymugineic acid (DMAS1) followed a similar pattern as NAS2 under -Fe condition, however, under alkaline conditions, all three genes were more highly expressed in Silero, as was the gene involved in Phys release (TOM1). The expression of the YSL gene, encoding for a product involved in Phys uptake, only increased in Minu II, under –Fe.

4. Discussion

4.1. Variability among sorghum genotypes in response to substrate alkalinity

Meeting food and energy demands in the near future will require expanding global crop production frontiers toward marginal lands. Sorghum is known to tolerate unfavorable environmental conditions, yet in saline/alkaline conditions seed germination and seedling growth and survival are compromised (Zhao et al., 2014). To study the physiological basis for such susceptibility required the identification of genotypes with contrasting alkalinity tolerance. Variability for this trait was explored in hydroponics, in a group of eight sorghum genotypes. Among them, Silero, a dual-purpose variety with high grain and biomass yield (https://inta.gob.ar/variedades/silero-inta-peman), had the best performance under high pH, in term of biomass accumulation and photosynthesis (Fig. 1A and B). On the other hand, Minu II, a variety of high potential to produce grain, biomass and stem juice as well as tolerant to drought and heat stress (https://inta.gob.ar/variedades/minu-ii-inta-peman), had very poor growth in alkaline medium, along with strongly reduced photosynthesis. These two contrasting genotypes were selected for further studies. Sudangrass, reported to be Fe-deficiency tolerant (Clark et al., 1988) was included in the subsequent experiments.

As plant response to alkaline substrates carried out in aerated nutrient solutions can only partially address the complexity of this stress (Luna et al., 2016), we confirmed the relative tolerance of the genotypes in a pot experiment with alkaline and neutral soil, where sudangrass and Silero showed a very similar degree of alkalinity tolerance, and higher than Minu II in terms of growth and carbon fixation.

Successful germination under soil salinity and/or alkalinity has been recognized as a key trait for breeding sorghum for these conditions (Zhao et al., 2014). Alkaline soil severely affected the percentage of emergence of Minu II, and to a lesser degree of Silero and sudangrass

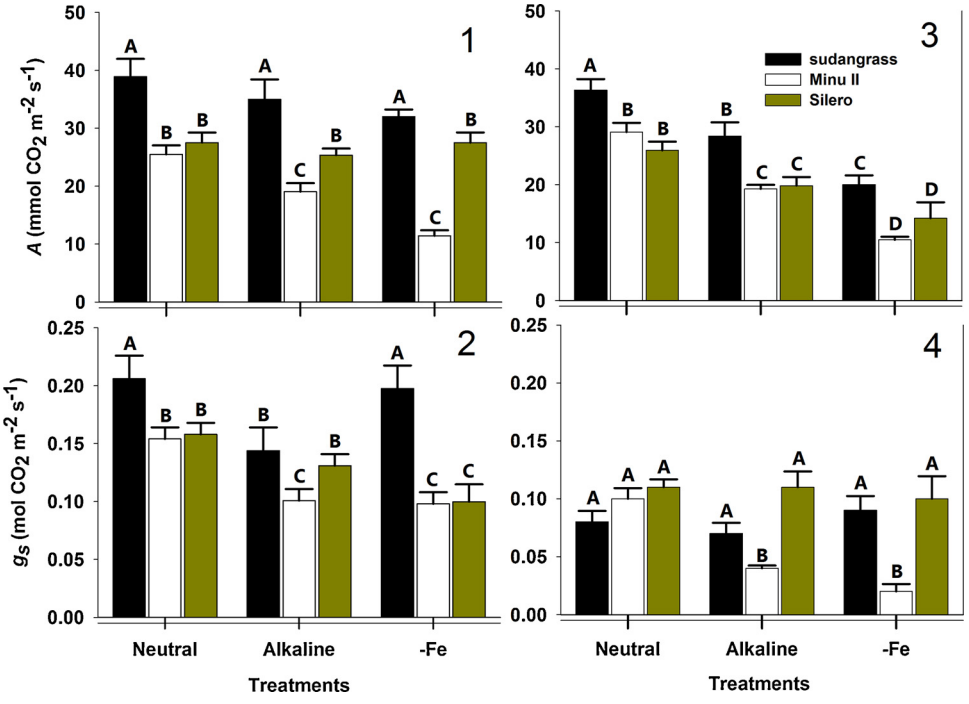

Fig. 5. Net carbon fixation and stomatal conductance in plants of *S. bicolor* (Minu II and Silero) and sudangrass growing in neutral, alkaline and Fe-deprived nutrient solutions. A and C. Net CO_2 assimilation rate (*A*). B and D, Stomatal conductance (*gs*). Measurements were taken on days 5 (A, B) and 15 (C, D) of treatment. Different letters indicate significant differences at $p < 0.05$, $n = 8$.

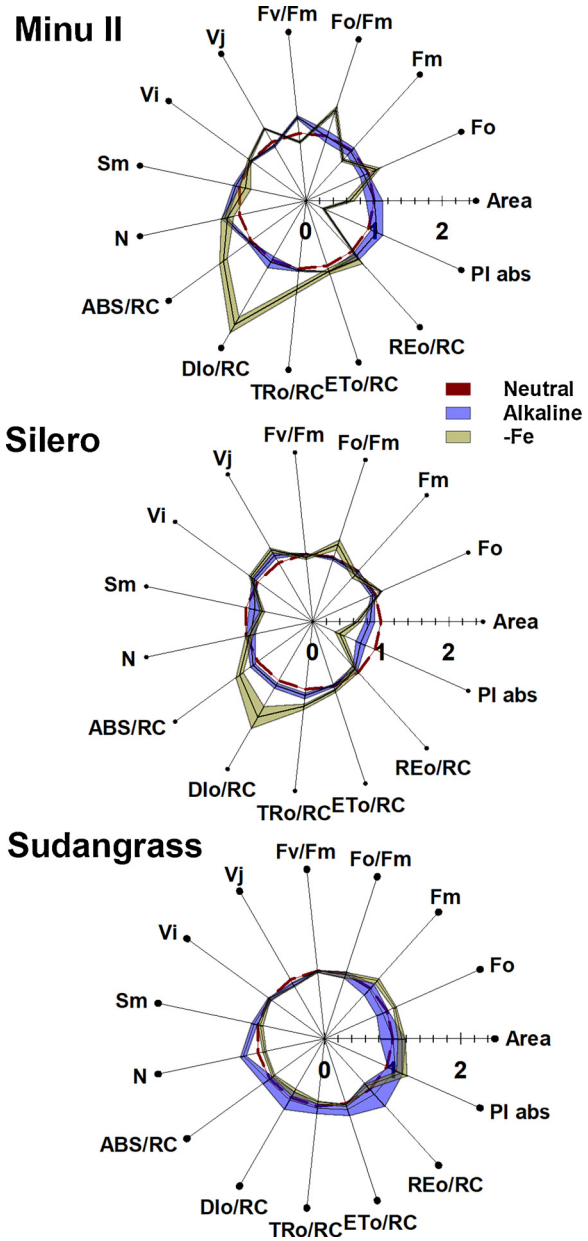

Fig. 6. Radar plot showing OJIP test parameters in plants of *S. bicolor* (Minu II and Silero) and sudangrass cultivated for 5 d in neutral, alkaline and Fe-deprived nutrient solutions. Parameter abbreviations and biological meaning are described in Supplementary Table 2.

(Supplementary Fig. 1), indicating that the relative alkalinity tolerance of the *Sorghum* genotypes, observed in hydroponics, agreed with alkalinity tolerance at the germination phase. In the case of salinity, tolerance at the germination stage may not predict tolerance at later developmental stages (Läuchli and Grattan, 2007). Nevertheless, the coincidence observed in this work between alkalinity tolerance at germination and at later vegetative growth deserves further exploration for the design of early screening tests.

4.1.1. Limited CO_2 fixation under alkaline conditions

4.1.1.1. Biochemical and stomatal conductance alterations. Carbon fixation can be negatively affected by reduced CO_2 diffusion through the stomata and the mesophyll (Flexas et al., 2004, 2007) or the alterations of photosynthetic metabolism (Lawlor and Cornic, 2002). In the current study, Minu II, Silero and sudangrass growing in soil with high pH (~9) showed reductions biomass accumulation and carbon fixation. The analysis of the A/C_i curves indicated that carbon fixation reactions were affected by the alkaline condition in all genotypes, but the effect in Minu II was more severe (Fig. 2). This was reflected in the reduced CO_2-saturated photosynthetic rate, V_{pr}, calculated from the horizontal asymptote of each A/Ci curve (Fig. 2D). Reduced V_{pr} may suggest decreased activity of either Rubisco or pyruvate orthophosphate dikinase (PPDK) (Furbank et al., 1997). PPDK is an abundant mesophyll-chloroplast enzyme involved in C4 photosynthesis. It plays an essential role in regenerating phosphoenolpyruvate (PEP), the primary cellular CO_2 acceptor molecule. This cannot be elucidated here, yet evidences suggest Rubisco is the main enzyme limiting C4 photosynthesis under abiotic stresses such as low temperature and salinity (Bernacchi et al., 2001; Crafts-Brandner and Salvucci, 2002). Under saturating light conditions, the metabolic control of C4 photosynthesis varies according to the internal CO_2 concentration (C_i) (Naidu and Long, 2004). At low C_i, as may occur under low stomatal conductance, phosphoenol pyruvate caboxylase (PEPc) activity controls the photosynthetic rate (Caemmerer, 2000; Collatz et al., 1992), while, at high C_i, ribulose 1,5-bisphosphate (RuBP) regeneration (limited by whole-chain electron transport) may also affect photosynthesis. We found difference among the genotypes in the extent that PEPc efficiency (CE) was affected by the alkaline soil (Fig. 2E). This effect may be related to the high exchangeable Na in the soil used for pot experiments. Tolerance of sorghum to salinity has been associated, among other traits, to restricted Na^+ accumulation in shoots (Lacerda et al., 2001). In this work, we observed high Na^+ accumulation in shoots of both Minu II and Silero, in contrast to sudangrass which successfully excluded it from shoots (Supplementary Fig. 2). Inhibition of PEPc has been shown to take place under high level of NaCl (100 mM) in *in-vitro* assays (Manetas, 2006). Intracellular Na^+ compartmentation, and protection provided by organic compatible solutes may contribute to avoid the negative consequences of high Na^+ concentrations in plant tissues (Munns and Tester, 2008). Hence, it remains to be determined whether these mechanisms are present in Silero and sudangrass.

At normal ambient CO_2 (~ 400 ppm), we observed limitation in stomatal conductance (g_s) only in Minu II (Fig. 5C). However, g_s reduction by itself does not seem to be the main reason for the lower carboxylation rate of Minu II. Rather, the elevated value C_i/C_a (high CO_2 concentration at the substomatal cavity; Fig. 2F) may also be a consequence of reduced carboxylation activity.

4.1.1.2. Damage to the structure and functions of PSII induced by alkalinity and Fe deprivation. Chlorophyll fluorescence analysis has been applied as a tool for characterization of plants for stress tolerance (Kalaji et al., 2017). Plants grown in Fe-deprived solution for five days showed alterations in most of the OJIP-test parameters while they were not evident in the alkaline substrate. Since Fe was completely absent in the Fe-deprived treatment, those results may suggest there is a tight Fe concentration threshold for effects to be expressed (as seen by the differences in chlorosis observed after 10 d of treatment in Fig. 4), and that it had not been yet attained after 5 d cultivation in alkaline substrate. Later sampling, on day 15 of treatment, indicated C fixation and stomatal conductance had been negatively influenced by alkalinity (Fig. 5C, D).

The absolute performance index (PI_{abs}), a recognized parameter for assessing early indication of abiotic stresses (Strasser et al., 2004), combines the photochemical and non photochemical properties as well as the density of active reaction centers per chlorophyll absorption in a single parameter (Chen et al., 2015). In Minu II and to a lesser extent in Silero, the PI_{abs} was significantly affected by Fe-deficit, possibly as a consequence of reductions of energy supply from light-harvesting pigments toward RCs, and/or disconnection among PSII antenna subunits (Morales et al., 2001).

Under photoinhibitory conditions, excess absorbed energy in the light-harvesting antenna complexes (LHCs) is dissipated as latent heat

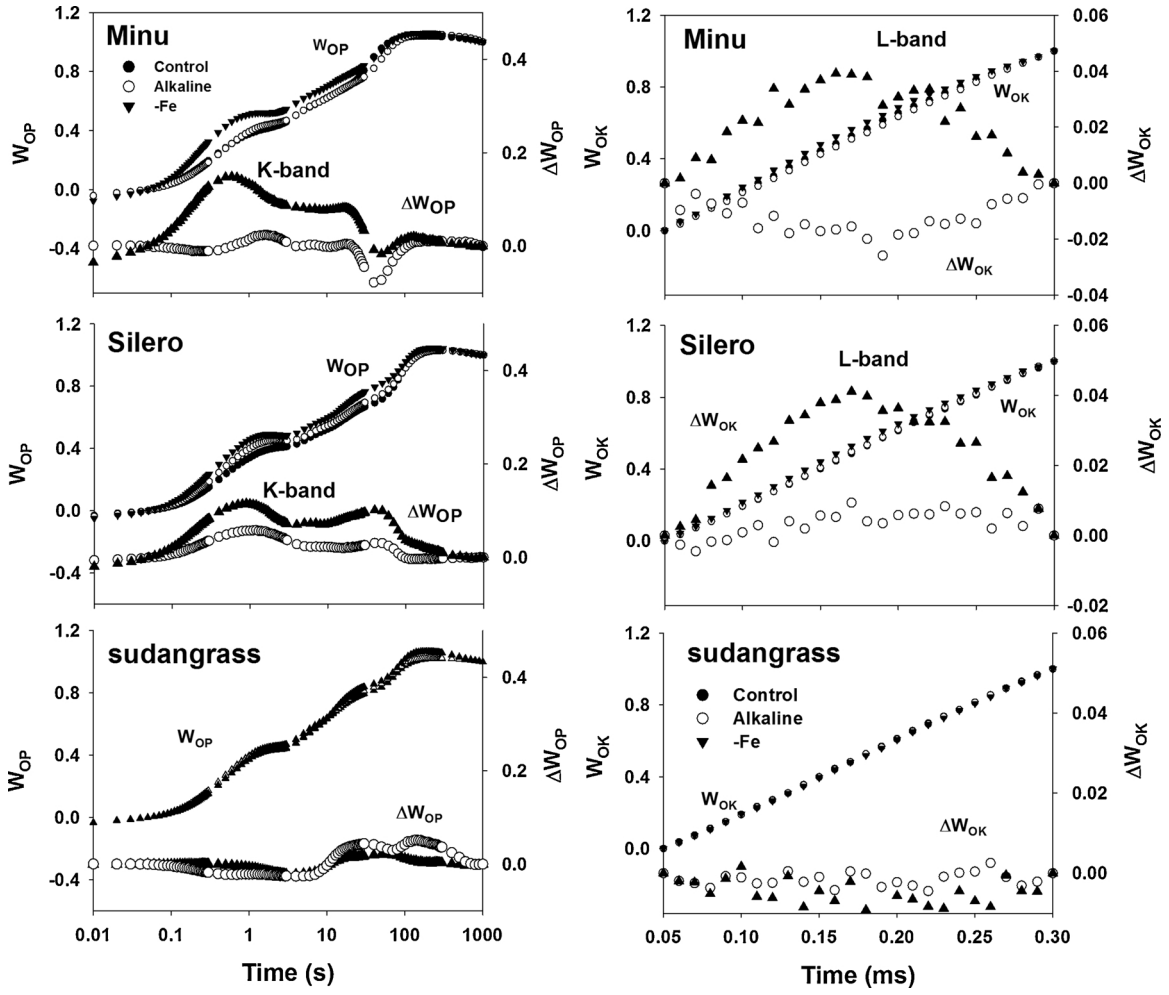

Fig. 7. Changes in the oxygen evolving complex (OEC, K band) and energetic connectivity of PSII units (L band) in plants of *S. bicolor* (Minu II and Silero) and sudangrass growing in neutral (black circles), alkaline (empty circles) and Fe-deprived (triangles) nutrient solutions. Left panels: W_{OP}: Normalized fluorescence kinetics from O (50 μs) to P step (300 ms). $\Delta W_{OP} = W_{OP(Treated)} - W_{OP(Control)}$, kinetics difference between treated and control plants, revealing the K-band. Right panels, W_{OK}: Normalized fluorescence kinetics from O (50 μs) to K step (300μs). $\Delta W_{OK} = W_{OK(Treated)} - W_{OK(Control)}$; kinetics difference between treated and control plants, revealing the L-band.

(Maxwell and Johnson, 2000). We speculate that such photoprotective mechanism (represented by the DIo/RC parameter; Figs. 6A and B) was still effective in Minu II and Silero due to the short exposure (5 days) to Fe absence. This would suggest, as hinted by the slight response of the Fv/Fm parameter, that stress is still incipient. Moreover, a significant increment in the antenna size (ABS/RC) was observed in Minu II and somewhat less in Silero, which may suggest another way of coping with excessive light energy. Such response is thought to be associated to the reduction of active RC (Srivastava et al., 1997). Furthermore, the variation in antenna size of PSII can also represent changes in the number of LHC complexes per RC, suggesting a decrease in the connectivity between antenna molecules and an increase in the number of inactive centers (Mathur et al., 2011).

A prominent K-band has been associated with a dissociation of the oxygen-evolving-complex (OEC) in *S. bicolor* under drought stress (Jedmowski et al., 2013). In this work, the K-band was more conspicuous in Minu II than Silero, and was not detected in sudangrass (Fig. 7). K bands were more marked under -Fe conditions, suggesting susceptibility to Fe deprivation was associated to disruptions in electron transport at the OEC.

Taken as a whole, these results indicate agreement between susceptibility to alkalinity and Fe deprivation in *S. bicolor* and suggest that alterations in PSII characteristics may be partially responsible for such susceptibility.

4.2. Expression of genes involved in phytosiderophores production, release and uptake

The main Fe mineral forms in soil are poorly soluble Fe (hydr) oxides, whose solubility is pH-dependent and decreases with increasing pH. The activities of living organisms that result in the acidification of the rhizosphere, such as the release of protons, organic acids and root respiration play important roles in mineral weathering. In addition, in nutrient-deficient conditions, plant roots produce exudates that contribute to mineral dissolution and Fe mobilization (Mimmo et al., 2014) and are critical for Fe acquisition. Specifically, under such conditions, grass roots release chelating substances collectively known as “phytosiderophores” (Phys) which are highly effective to mobilize the sparingly soluble Fe^{+3} (Strategy II, as defined by Römheld, 1987). Overexpression of genes involved in Phys synthesis, release and uptake, has been widely investigated in other species such as barley, maize, rice, etc. (Nozoye et al., 2011). However, very little is known about the expression of such genes in sorghum and there are no records in sudangrass. Increases in the activities of both nicotianamine synthase (NAS) and nicotianamine aminotransferase (NAAT) genes are crucial for the enhanced production of MAs by Fe-deficient graminaceous plants, and therefore for Fe deficiency tolerance (Higuchi et al., 1996).It is interesting that while the expression of both genes increased in Minu II and Silero under Fe-deficiency, the increase observed in alkaline

medium in these as well as in DMAS1 and TOM1 was greater in Silero. This could indicate that this genotype was responding earlier than Minu II to alkalinity-associated Fe deficiencies and this response could contribute to account for its higher alkalinity tolerance. This response could also contribute to explaining the lower effects of Fe-deprivation observed in the development of induced chlorosis and in the alterations of PSII activity and components.

On the other hand, Fe is required by many enzymes involved in N and S assimilation, such as nitrate and nitrite reductases, glutamate synthase, sulfite reductase, etc. (Balk and Lobréaux, 2005). Thus, prolonged Fe deficiency may have significantly reduced NO_3^- and SO_4^{2-} assimilation (Fig. 3). In Fe-deficient barley leaves, down-regulation of genes responsible for S assimilation and SO_4 transport was observed (Higuchi et al., 2011); at the same time, such S accumulation was related to the its use for the synthesis of methionine, which is the precursor of Phys.

These results indicate that sudangrass was more efficient in Fe utilization; as photochemical reactions were not affected by either alkaline or –Fe conditions they may imply it was not perceiving Fe-deficiency stress, and, thus, the genes for Phys synthesis and transport were activated to a lesser extent than in the other genotypes. In *S. bicolor*, they suggest that the lower expression of these genes in Minu II may be related to its sensitivity to alkalinity conditions associated to reduced Fe availability, leading to alteration in photochemical and biochemical reactions involving Fe.

Positive associations between Fe acquisition mechanisms and alkalinity tolerance have recently been reported in *Lotus*, a plant with Strategy I Fe uptake mechanism (Babuin et al., 2014). In rice, a species with strategy II, alkalinity tolerance has also been associated to Fe uptake capacity (Li et al., 2016). In *Petunia*, another species with Strategy I, increased alkalinity tolerance was observed when transformed with the HvYS1 transporter gene derived from barley (Murata et al., 2015). Our results in sorghum provide further support to the notion that Fe acquisition mechanisms contribute to alkalinity tolerance.

4.3. An integrated picture of early responses to alkalinity and Fe-deprivation

A principal components analysis (PCA) was applied to the results obtained on day 5 of the -Fe and alkalinity treatments (Experiment 3), including photosynthetic and fluorescence variables, gene expression and Fe^{2+} concentration. Eight components with eigenvalues of 11.5, 5.53, 4.55, 0.97, 0.57, 0.5, 0.24, 0.15, respectively, were extracted. The first three accounted for approximately 90% of the total variance. The first two components described 70.9% of the total variance and the corresponding biplot is shown in Fig. 8. The first component (horizontal axis) placed on the right side all the genotypes in the control treatment, along with sudangrass in alkalinity and -Fe, and Silero in alkalinity. Minu II, both in alkalinity and -Fe, and Silero in -Fe were located on the opposite side. This distribution illustrates that sudangrass was less affected by the two stress conditions (alkalinity and -Fe) than the other two genotypes, and that Minu II was the most susceptible among them. The position of the genotypes along the left side of the PC1 axis shows that responses to the -Fe treatment were more marked than to alkalinity, as has been discussed earlier. The sensitivity of Minu II to alkalinity and -Fe was negatively associated to Fe^{2+} concentrations, and to the expression of the five genes tested, which codify for proteins involved in Phys synthesis and transport. It was also negatively associated to carbon fixation and stomatal conductance. Sensitivity to both alkalinity and -Fe conditions was positively associated to alterations in most fluorescence kinetics parameters, which, in turn, were also negatively associated to plant Fe^{2+} concentrations.

The hypothesis that guided this research was that alkalinity tolerance in sorghum is related to Fe-deficiency tolerance and its underlying mechanisms. Our results provide support to this hypothesis and to the concept that initial alkalinity tolerance expression in sorghum may be

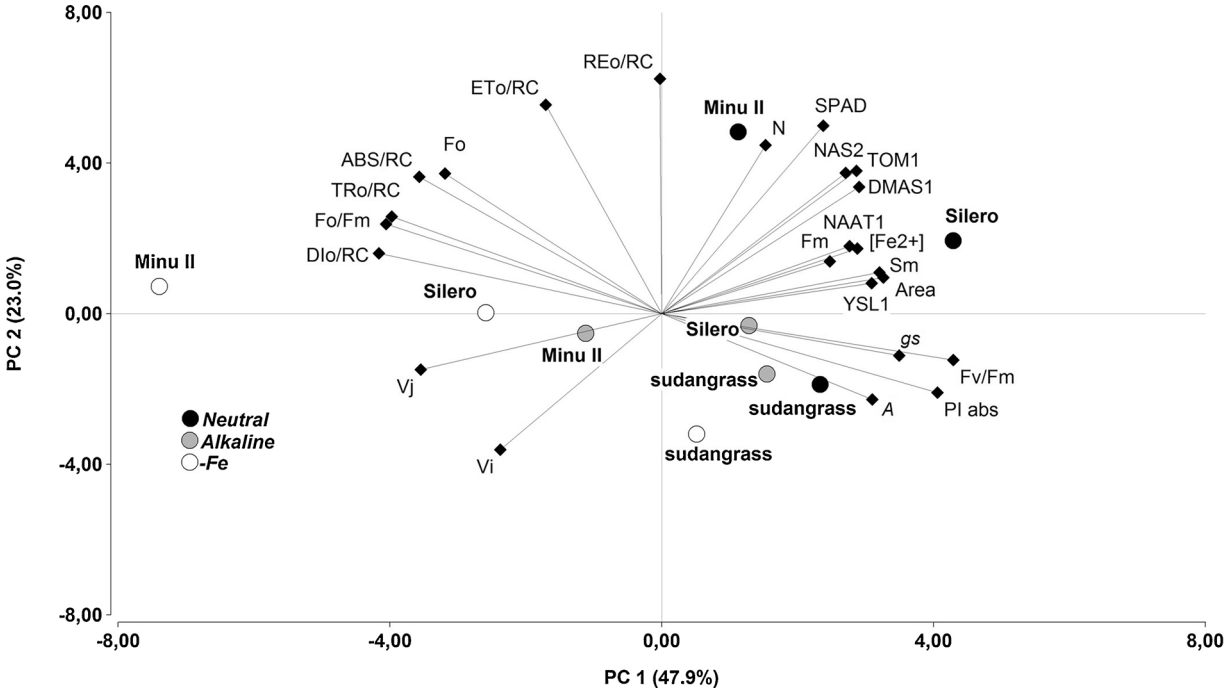

Fig. 8. Biplot of a Principal Component Analysis including results from *S. bicolor* (Minu II and Silero) and sudangrass plants cultivated in neutral, alkaline and Fe-deprived substrate for 5d. Black circles: genotypes in neutral substrate, grey circles: genotypes in alkaline substrate, empty circles: genotypes in -Fe substrate. Vectors orientation represent the correlation among the variables (♦) and their length, the weight to the contribution for explaining the variance. OJIP variables: ABS/RC, TRo/RC, ETo/RC, DIo/RC, REo/RC, V_i, Vj, PI abs, Fv/Fm, Fo/Fm, Fo, Fm, Area, Sm and N (see biological meaning and description in Supplementary Table 2); *gs*: stomatal conductance; *A* (Net CO_2 assimilation rate); Phys genes: NAS2, NAAT1, DMAS1, TOM1, YSL1; SPAD index (SPAD); [Fe^{2+}]: active iron concentration in leaves. Coffenetic correlation coefficient 0.929.

related to Fe^{2+}uptake mechanisms and metabolism, specifically affecting PSII functionality. From an agricultural point of view, identifying some of the components in the complex trait of alkalinity tolerance could contribute to breeding plants for alkaline substrates and to the design of agronomic management practices aimed at increasing Fe availability in alkaline substrates.

Acknowledgments

The help of Daniela Gómez with greenhouse and laboratory work and statistics consultation with Cecilia Bruno (CONICET) are sincerely appreciated. Funding from MINCYT (PICT 2012 00498 and PICT 2016 1136) and INTA (PNAGUA 1133032 and PNPA 11260713) is gratefully acknowledged. The authors are indebted to Oscar Pemán SA for continued support. Soil analyses were carried out by Laboratorio Jarsum, Córdoba, Argentina.

Appendix A. Supplementary data

Supplementary material related to this article can be found, in the online version, at doi:https://doi.org/10.1016/j.envexpbot.2018.06.030.

References

Babuin, M.F., Campestre, M.P., Rocco, R., Bordenave, C.D., Escaray, F.J., Antonelli, C., Calzadilla, P., Gárriz, A., Serna, E., Carrasco, P., Ruiz, O.A., Menendez, A.B., 2014. Response to long-term $NaHCO_3$-derived alkalinity in model *Lotus japonicus* ecotypes Gifu B-129 and Miyakojima MG-20: transcriptomic profiling and physiological characterization. PLoS One 9, e97106. http://dx.doi.org/10.1371/journal.pone.0097106.

Balk, J., Lobréaux, S., 2005. Biogenesis of iron–sulfur proteins in plants. Trends Plant Sci. 10, 324–331. http://dx.doi.org/10.1016/J.TPLANTS.2005.05.002.

Bellasio, C., Beerling, D.J., Griffiths, H., 2016. An Excel tool for deriving key photosynthetic parameters from combined gas exchange and chlorophyll fluorescence: theory and practice. Plant Cell Environ. 39, 1180–1197. http://dx.doi.org/10.1111/pce.12560.

Bernacchi, C.J., Singsaas, E.L., Pimentel, C., Portis Jr., A.R., Long, S.P., 2001. Improved temperature response functions for models of Rubisco-limited photosynthesis. Plant Cell Environ. 24, 253–259. http://dx.doi.org/10.1111/j.1365-3040.2001.00668.x.

Bussotti, F., 2010. Assessment of stress conditions in Quercus ilex L. leaves by O-J-I-P chlorophyll a fluorescence analysis. Plant Biosyst. 138, 101–109. http://dx.doi.org/10.1080/11263500412331283708.

Caemmerer, Svon, 2000. Biochemical Models of Leaf Photosynthesis. CSIRO Publishing, Collingwood.

Campestre, M.P., Antonelli, C., Calzadilla, P.I., Maiale, S.J., Rodríguez, A.A., Ruiz, O.A., 2016. The alkaline tolerance in *Lotus japonicus* is associated with mechanisms of iron acquisition and modification of the architectural pattern of the root. J. Plant Physiol. 206, 40–48. http://dx.doi.org/10.1016/J.JPLPH.2016.09.005.

Chaves, M.M., Flexas, J., Pinheiro, C., 2009. Photosynthesis under drought and salt stress: regulation mechanisms from whole plant to cell. Ann. Bot. 103, 551–560. http://dx.doi.org/10.1093/aob/mcn125.

Chen, S., Kang, Y., Zhang, M., Wang, X., Strasser, R.J., Zhou, B., Qiang, S., 2015. Differential sensitivity to the potential bioherbicide tenuazonic acid probed by the JIP-test based on fast chlorophyll fluorescence kinetics. Environ. Exp. Bot. 112, 1–15. http://dx.doi.org/10.1016/j.envexpbot.2014.11.009.

Clark, A., 2007. Managing Cover Crops Profitably, third ed. Sustainable Agriculture Network, Maryland. http://dx.doi.org/10.1007/s13398-014-0173-7.2. Handbook series.

Clark, R.B., Römheld, V., Marschner, H., 1988. Iron uptake and phytosiderophore release by roots of sorghum genotypes. J. Plant Nutr. 11, 663–676. http://dx.doi.org/10.1080/01904168809363832.

Collatz, G., Ribas-Carbo, M., Berry, J., 1992. Coupled photosynthesis-stomatal conductance model for leaves of C4 plants. Funct. Plant Biol. 19, 519–538. http://dx.doi.org/10.1071/PP9920519.

Crafts-Brandner, S.J., Salvucci, M.E., 2002. Sensitivity of photosynthesis in a C4 plant, maize, to heat stress. Plant Physiol. 129, 1773–1780. http://dx.doi.org/10.1104/pp.002170.

Curie, C., Panaviene, Z., Loulergue, C., Dellaporta, S.L., Briat, J.-F., Walker, E.L., 2001. Maize yellow stripe1 encodes a membrane protein directly involved in Fe(III) uptake. Nature 409, 346–349. http://dx.doi.org/10.1038/35053080.

Curie, C., Cassin, G., Couch, D., Divol, F., Higuchi, K., Le Jean, M., Misson, J., Schikora, A., Czernic, P., Mari, S., 2009. Metal movement within the plant: contribution of nicotianamine and yellow stripe 1-like transporters. Ann. Bot. 103, 1–11. http://dx.doi.org/10.1093/aob/mcn207.

Di Rienzo, J.A., Casanoves, F., Balzarini, M.G., Gonzalez, L., Tablada, M., Robledo, C.W., 2011. InfoStat. last update 11 March 2018. http://www.infostat.com.ar/.

FAO, ITPS, 2015. Status of the World's Soil Resources (sWSR) - Main Report. Food Agric. Organ. United Nations Intergov. Tech. Panel Soils, Rome, Italy.

Farquhar, G.D., von Caemmerer, S., Berry, J.A., 1980. A biochemical model of photosynthetic CO_2 assimilation in leaves of C3 species. Planta 149, 78–90. http://dx.doi.org/10.1007/BF00386231.

Flexas, J., Bota, J., Loreto, F., Cornic, G., Sharkey, T.D., 2004. Diffusive and metabolic limitations to photosynthesis under drought and salinity in C3 plants. Plant Biol. 6, 269–279. http://dx.doi.org/10.1055/s-2004-820867.

Flexas, J., Diaz-Espejo, A., Galmés, J., Kaldenhoff, R., H, Medrano, Ribas-Carbo, M., 2007. Rapid variations of mesophyll conductance in response to changes in CO_2 concentration around leaves. Plant. Cell Environ. 30, 1284–1298. http://dx.doi.org/10.1111/j.1365-3040.2007.01700.x.

Furbank, R.T., Chitty, J.A., Jenkins, C.L.D., Taylor, W.C., Trevanion, J., von Caemmerer, S., Ashton, R., 1997. Genetic manipulation of key photosynthetic enzymes in the C4 plant Flaveria bidentis. Funct. Plant Biol. 24, 477–485. http://dx.doi.org/10.1071/PP97028.

Gururani, M.A., Venkatesh, J., Ganesan, M., Strasser, R.J., Han, Y., Kim, J.-I., Lee, H.-Y., Song, P.-S., 2015. In vivo assessment of cold tolerance through chlorophyll-A fluorescence in transgenic Zoysiagrass expressing mutant phytochrome A. PLoS One 10, e0127200. http://dx.doi.org/10.1371/journal.pone.0127200.

Hell, R., Stephan, U.W., 2003. Iron uptake, trafficking and homeostasis in plants. Planta 216, 541–551. http://dx.doi.org/10.1007/s00425-002-0920-4.

Higuchi, K., Kanazawa, K., Nishizawa, N.-K., Chino, M., Mori, S., 1994. Purification and characterization of nicotianamine synthase from Fe-deficient barley roots. Plant Soil 165, 173–179. http://dx.doi.org/10.1007/BF00008059.

Higuchi, K., Kanazawa, K., Nishizawa, N.-K., Mori, S., 1996. The role of nicotianamine synthase in response to Fe nutrition status in Gramineae. Plant Soil 178, 171–177. http://dx.doi.org/10.1007/BF00011580.

Higuchi, K., Saito, A., Mikami, Y., Miwa, E., 2011. Modulation of macronutrient metabolism in barley leaves under iron-deficient condition. Soil Sci. Plant Nutr. 57, 233–247. http://dx.doi.org/10.1080/00380768.2011.564574.

Hoagland, D.R., Arnon, D.I., 1950. The water-culture method for growing plants without soil. Circular, 2nd ed. California Agricultural Experiment Station. College of Agriculture, University of California, California, USA.

Inoue, H., Takahashi, M., Kobayashi, T., Suzuki, M., Nakanishi, H., Mori, S., Nishizawa, N.K., 2008. Identification and localisation of the rice nicotianamine aminotransferase gene OsNAAT1 expression suggests the site of phytosiderophore synthesis in rice. Plant Mol. Biol. 66, 193–203. http://dx.doi.org/10.1007/s11103-007-9262-8.

Jedmowski, C., Ashoub, A., Brüggemann, W., 2013. Reactions of Egyptian landraces of *Hordeum vulgare* and *Sorghum bicolor* to drought stress, evaluated by the OJIP fluorescence transient analysis. Acta Physiol. Plant 35, 345–354. http://dx.doi.org/10.1007/s11738-012-1077-9.

Kalaji, H.M., Schansker, G., Ladle, R.J., Goltsev, V., Bosa, K., Allakhverdiev, S.I., Brestic, M., Bussotti, F., Calatayud, A., Dąbrowski, P., Elsheery, N.I., Ferroni, L., Guidi, L., Hogewoning, S.W., Jajoo, A., Misra, A.N., Nebauer, S.G., Pancaldi, S., Penella, C., Poli, D., Pollastrini, M., Romanowska-Duda, Z.B., Rutkowska, B., Serôdio, J., Suresh, K., Szulc, W., Tambussi, E., Yanniccari, M., Zivcak, M., 2014. Frequently asked questions about in vivo chlorophyll fluorescence: practical issues. Photosynth. Res. 122, 121–158. http://dx.doi.org/10.1007/s11120-014-0024-6.

Kalaji, H.M., Račková, L., Paganová, V., Swoczyna, T., Rusinowski, S., Sitko, K., 2017. Can chlorophyll-a fluorescence parameters be used as bio-indicators to distinguish between drought and salinity stress in *Tilia cordata* Mill? Environ. Exp. Bot. 152, 149–157. http://dx.doi.org/10.1016/j.envexpbot.2017.11.001.

Kaňa, R., Govindjee, 2016. Role of ions in the regulation of light-harvesting. Front. Plant Sci. 7, 1849. http://dx.doi.org/10.3389/fpls.2016.01849.

Kanazawa, K., Higuchi, K., Nishizawa, N.-K., Fushiya, S., Mori, S., 1995. Detection of two distinct isozymes of nicotianamine aminotransferase in Fe-deficient barley roots. J. Exp. Bot. 46, 1241–1244. http://dx.doi.org/10.1093/jxb/46.9.1241.

Kawai, S., Takagi, S., Sato, Y., 1988. Mugineic acid-family phytosiderophores in root--secretions of barley, corn and sorghum varieties. J. Plant Nutr. 11, 633–642. http://dx.doi.org/10.1080/01904168809363829.

Kobayashi, T., Nishizawa, N.K., 2012. Iron uptake, translocation, and regulation in higher plants. Annu. Rev. Plant Biol. 63, 131–152. http://dx.doi.org/10.1146/annurev-arplant-042811-105522.

Kobayashi, T., Nakanishi, H., Takahashi, M., Mori, S., Nishizawa, N.K., 2008. Generation and field trials of transgenic rice tolerant to iron deficiency. Rice 1, 144–153. http://dx.doi.org/10.1007/s12284-008-9011-x.

Kobayashi, T., Nakanishi Itai, R., Nishizawa, N.K., 2014. Iron deficiency responses in rice roots. Rice 7, 27. http://dx.doi.org/10.1186/s12284-014-0027-0.

Lacerda, C.F., De Cambraia, J., Cano, M.A.O., Ruiz, H.A., 2001. Plant growth and solute accumulation and distribution in two sorghum genotypes, under NaCl stress. Rev. Bras. Fisiol. Veg. 13, 270–284.

Läuchli, A., Grattan, S.R., 2007. Plant growth and development under salinity stress. In: Jenks, M.A., Hasegawa, P.M., Jain, S.M. (Eds.), Advances in Molecular Breeding Toward Drought and Salt Tolerant Crops. Springer, Netherlands, Dordrecht, pp. 1–32. http://dx.doi.org/10.1007/978-1-4020-5578-2_1.

Lawlor, W.D., Cornic, D.G., 2002. Photosynthetic carbon assimilation and associated metabolism in relation to water deficits in higher plants. Plant. Cell Environ. 25, 275–294. http://dx.doi.org/10.1046/j.0016-8025.2001.00814.x.

Li, Q., Yang, A., Zhang, W.-H., 2016. Efficient acquisition of iron confers greater tolerance to saline-alkaline stress in rice (*Oryza sativa* L.). J. Exp. Bot. 67, 6431–6444. http://dx.doi.org/10.1093/jxb/erw407.

Luna, D.F., Aguirre, A., Pittaro, G., Bustos, D., Ciacci, B., Taleisnik, E., 2016. Nutrient deficiency and hypoxia as constraints to *Panicum coloratum* growth in alkaline soils. Grass Forage Sci. 72, 640–653. http://dx.doi.org/10.1111/gfs.12263.

Mamedov, M., Govindjee, Nadtochenko, V., Semenov, A., 2015. Primary electron transfer processes in photosynthetic reaction centers from oxygenic organisms. Photosynth.

Res. 125, 51–63. http://dx.doi.org/10.1007/s11120-015-0088-y.
Manetas, Y., 2006. Are-examination of NaCl effects on phosphoenolpyruvate carboxylase at high (physiological) enzyme concentrations. Physiol. Plant 78, 225–229. http://dx.doi.org/10.1111/j.1399-3054.1990.tb02085.x.
Marschner, H., 1995. 16 - Adaptation of plants to adverse chemical soil conditions. In: Marschner, H. (Ed.), Mineral Nutrition of Higher Plants (Second Edition). Academic Press, London, pp. 596–680. http://dx.doi.org/10.1016/B978-012473542-2/50018-3.
Marschner, H., Römheld, V., Kissel, M., 1986. Different strategies in higher plants in mobilization and uptake of iron. J. Plant Nutr. 9, 695–713. http://dx.doi.org/10.1080/01904168609363475.
Mathur, S., Allakhverdiev, S.I., Jajoo, A., 2011. Analysis of high temperature stress on the dynamics of antenna size and reducing side heterogeneity of Photosystem II in wheat leaves (*Triticum aestivum*). Biochim. Biophys. Acta - Bioenerg. 1807, 22–29. http://dx.doi.org/10.1016/j.bbabio.2010.09.001.
Maxwell, K., Johnson, G.N., 2000. Chlorophyll fluorescence—a practical guide. J. Exp. Bot. 51, 659–668. http://dx.doi.org/10.1093/jexbot/51.345.659.
Mengel, K., Breininger, M.T., Bübl, W., 1984. Bicarbonate, the most important factor inducing iron chlorosis in vine grapes on calcareous soil. Plant Soil 81, 333–344. http://dx.doi.org/10.1007/BF02323048.
Mikami, Y., Saito, A., Miwa, E., Higuchi, K., 2011. Allocation of Fe and ferric chelate reductase activities in mesophyll cells of barley and sorghum under Fe-deficient conditions. Plant Physiol. Biochem. 49, 513–519. http://dx.doi.org/10.1016/j.plaphy.2011.01.009.
Mimmo, T., Del Buono, D., Terzano, R., Tomasi, N., Vigani, G., Crecchio, C., Pinton, R., Zocchi, G., Cesco, S., 2014. Rhizospheric organic compounds in the soil–microorganism–plant system: their role in iron availability. Eur. J. Soil Sci. 65, 629–642. http://dx.doi.org/10.1111/ejss.12158.
Morales, F., Moise, N., Quílez, R., Abadía, A., Abadía, J., Moya, I., 2001. Iron deficiency interrupts energy transfer from a disconnected part of the antenna to the rest of Photosystem II. Photosynth. Res. 70, 207–220. http://dx.doi.org/10.1023/a:1017965229788.
Mori, S., 1999. Iron acquisition by plants. Curr. Opin. Plant Biol. 2, 250–253. http://dx.doi.org/10.1016/S1369-5266(99)80043-0.
Munns, R., Tester, M., 2008. Mechanisms of salinity tolerance. Annu. Rev. Plant Biol. 59, 651–681. http://dx.doi.org/10.1146/annurev.arplant.59.032607.092911.
Murata, Y., Itoh, Y., Iwashita, T., Namba, K., 2015. Transgenic Petunia with the iron(III)-phytosiderophore transporter gene acquires tolerance to iron deficiency in alkaline environments. PLoS One 10, e0120227. http://dx.doi.org/10.1371/journal.pone.0120227.
Naidu, S.L., Long, S.P., 2004. Potential mechanisms of low-temperature tolerance of C4 photosynthesis in *Miscanthus* × *giganteus*: an in vivo analysis. Planta 220, 145–155. http://dx.doi.org/10.1007/s00425-004-1322-6.
Nozoye, T., Nagasaka, S., Kobayashi, T., Takahashi, M., Sato, Y., Sato, Y., Uozumi, N., Nakanishi, H., Nishizawa, N.K., 2011. Phytosiderophore efflux transporters are crucial for iron acquisition in graminaceous plants. J. Biol. Chem. 286, 5446–5454. http://dx.doi.org/10.1074/jbc.M110.180026.
Oukarroum, A., El Madidi, S., Schansker, G., Strasser, R.J., 2007. Probing the responses of barley cultivars (*Hordeum vulgare* L.) by chlorophyll a fluorescence OLKJIP under drought stress and re-watering. Environ. Exp. Bot. 60, 438–446. http://dx.doi.org/10.1016/j.envexpbot.2007.01.002.
Pfaffl, M.W., Horgan, G.W., Dempfle, L., 2002. Relative expression software tool (REST(C)) for group-wise comparison and statistical analysis of relative expression results in real-time PCR. Nucleic Acids Res. 30, e36. http://dx.doi.org/10.1093/nar/30.9.e36.
Rahman, M.M., Govindarajulu, Z., 1997. A modification of the test of Shapiro and Wilk for normality. J. Appl. Stat. 24, 219–236. http://dx.doi.org/10.1080/02664769723828.
Rao, P.S., Vinutha, K.S., Kumar, G.S.A., Chiranjeevi, T., Uma, A., Lal, P., Prakasham, R.S., Singh, H.P., Rao, R.S., Chopra, S., Jose, S., 2016. Sorghum: a multipurpose bioenergy crop. In: Ciampitti, I., Prasad, V. (Eds.), Sorghum: State of the Art and Future Perspectives. American Society of Agronomy and Crop Science Society of America, Inc., Madison, WI. http://dx.doi.org/10.2134/agronmonogr58.2014.0074.
Reddy, S.P., 2017. Sorghum, *Sorghum bicolor* (L.) Moench. In: Patil, J.V. (Ed.), Millets and Sorghum. John Wiley & Sons, Ltd, pp. 1–48. http://dx.doi.org/10.1002/9781119130765.ch1.
Reddy, S.P., Srinivas Reddy, D., Sivasakthi, K., Bhatnagar-Mathur, P., Vadez, V., Sharma, K.K., 2016. Evaluation of Sorghum [*Sorghum bicolor* (L.)] reference genes in various tissues and under abiotic stress conditions for quantitative real-time PCR data normalization. Front. Plant Sci. 7, 529. http://dx.doi.org/10.3389/fpls.2016.00529.
Rengasamy, P., Tavakkoli, E., McDonald, G.K., 2016. Exchangeable cations and clay dispersion: net dispersive charge, a new concept for dispersive soil. Eur. J. Soil Sci. 67, 659–665. http://dx.doi.org/10.1111/ejss.12369.
Roháček, K., Soukupová, J., Bartak, M., 2008. Chlorophyll fluorescence: a wonderful tool to study plant physiology and plant stress. In: Schoefs, B. (Ed.), Plant Cell Compartments. Research Signpost, India, pp. 41–104.
Römheld, V., 1987. Different strategies for iron acquisition in higher plants. Physiol. Plant 70, 231–234. http://dx.doi.org/10.1111/j.1399-3054.1987.tb06137.x.
Römheld, V., Marschner, H., 1990. Genotypical differences among graminaceous species in release of phytosiderophores and uptake of iron phytosiderophores. Plant Soil 123, 147–153. http://dx.doi.org/10.1007/BF00011260.
Rooney, W.L., 2014. Sorghum. In: Karlen, D.L. (Ed.), Cellulosic Energy Cropping Systems. John Wiley & Sons, Ltd, United Kingdom, pp. 109–129. http://dx.doi.org/10.1002/9781118676332.ch7.
Singh, K., Chino, M., Nishizawa, N.K., Ohata, T., Mori, S., 1993. Genotypic variation among Indian graminaceous species with respect to phytosiderophore secretion. In: Randall, P.J., Delhaize, E., Richards, R.A., Munns, R. (Eds.), Genetic Aspects of Plant Mineral Nutrition. Springer, Netherlands, Dordrecht, pp. 335–339. http://dx.doi.org/10.1007/978-94-011-1650-3_41.
Srivastava, A., Guissé, B., Greppin, H., Strasser, R.J., 1997. Regulation of antenna structure and electron transport in Photosystem II of *Pisum sativum* under elevated temperature probed by the fast polyphasic chlorophyll a fluorescence transient: OKJIP. Biochim. Biophys. Acta - Bioenerg. 1320, 95–106. http://dx.doi.org/10.1016/S0005-2728(97)00017-0.
Strasser, R.J., Srivastava, A., 1995. Polyphasic chlorophyll a fluorescence transient in plants and cyanobacteria. Photochem. Photobiol. 61, 32–42. http://dx.doi.org/10.1111/j.1751-1097.1995.tb09240.x.
Strasser, R.J., Tsimilli-Michael, M., Srivastava, A., 2004. Analysis of the chlorophyll a fluorescence transient. In: Papageorgiou, G.C., Govindjee (Eds.), Chlorophyll a Fluorescence: A Signature of Photosynthesis. Springer, Netherlands, Dordrecht, pp. 321–362. http://dx.doi.org/10.1007/978-1-4020-3218-9_12.
Svec, D., Tichopad, A., Novosadova, V., Pfaffl, M.W., Kubista, M., 2015. How good is a PCR efficiency estimate: recommendations for precise and robust qPCR efficiency assessments. Biomol. Detect. Quantif. 3, 9–16. http://dx.doi.org/10.1016/j.bdq.2015.01.005.
Tan, Z.-H., Wu, Z.-X., Hughes, A.C., Schaefer, D., Zeng, J., Lan, G.-Y., Yang, C., Tao, Z.-L., Chen, B.-Q., Tian, Y.-H., Song, L., Jatoi, M.T., Zhao, J.-F., Yang, L.-Y., 2017. On the ratio of intercellular to ambient CO_2 (C_i/C_a) derived from ecosystem flux. Int. J. Biometeorol. 61, 2059–2071. http://dx.doi.org/10.1007/s00484-017-1403-4.
Ubierna, N., Sun, W.E.I., Kramer, D.M., Cousins, A.B., 2013. The efficiency of C4 photosynthesis under low light conditions in *Zea mays*, *Miscanthus x giganteus* and *Flaveria bidentis*. Plant. Cell Environ. 36, 365–381. http://dx.doi.org/10.1111/j.1365-3040.2012.02579.x.
Yin, X., Sun, Z., Struik, P.C., Van Der Putten, P.E.L., Van Ieperen, W.I.M., Harbinson, J., 2011. Using a biochemical C4 photosynthesis model and combined gas exchange and chlorophyll fluorescence measurements to estimate bundle-sheath conductance of maize leaves differing in age and nitrogen content. Plant. Cell Environ. 34, 2183–2199. http://dx.doi.org/10.1111/j.1365-3040.2011.02414.x.
Zhao, Y., Lu, Z., He, L., 2014. Effects of saline-alkaline stress on seed germination and seedling growth of *Sorghum bicolor* (L.) Moench. Appl. Biochem. Biotechnol. 173, 1680–1691. http://dx.doi.org/10.1007/s12010-014-0956-5.
Zhou, H., Akcay, E., Helliker, B., 2017. Deriving C4 Photosynthesis Parameters by Fitting Intensive A/Ci Curves. bioRxiv. http://dx.doi.org/10.1101/153072.